Electric Power Systems Research 173 (2019) 122–134

Contents lists available at ScienceDirect

Electric Power Systems Research

journal homepage: www.elsevier.com/locate/epsr

# The breakthrough phase of lightning attachment process: From collision of opposite-polarity streamers to hot-channel connection

V.A. Rakov[a,b,*], M.D. Tran[a,c]

[a] Department of Electrical and Computer Engineering, University of Florida, Gainesville, FL 32611, USA
[b] Moscow Institute of Electronics and Mathematics, National Research University Higher School of Economics, Moscow 101000, Russia
[c] Rhombus Power Inc., Gainesville, FL 32601, USA

ARTICLE INFO

Keywords:
Lightning
Long sparks
Breakthrough phase
Common streamer zone
Attachment process
Final jump

ABSTRACT

Recent progress in studying the breakthrough phase (BTP) of the attachment process in lightning and long sparks is reviewed. The main focus is on the new insights gained from recent observations for 3 types of electric discharges: natural lightning (Nag et al., 2012; Tran and Rakov, 2017a,c), rocket-and-wire triggered lightning (Howard et al., 2010; Hill et al., 2016), and long sparks (Kostinskiy et al., 2016). The BTP (also known as the final jump) starts when the poorly-conducting streamer zones, developing ahead of the hot channels of negative downward leader (DL) and positive upward connecting leader (UCL), come in contact and a common streamer zone (CSZ) is formed. The beginning of BTP (establishment of CSZ) is usually marked by an abrupt current rise, a burst of dE/dt pulses (referred to as leader burst or LB), and hard X-ray emission. During the BTP, hot channels of both DL and UCL extend toward each other inside the CSZ, resulting in its shrinking, until the high-impedance CSZ is eliminated and low-impedance connection of DL to the grounded object is established. The process of bridging of CSZ by hot leader channels is accompanied by the formation of slow front (SF) in the channel current and in electric and magnetic field waveforms at both close and far distances from the channel. Attempted or relatively weak hot-channel connections producing current surges and associated field pulses superimposed on the SF (SF pulses) can occur. The SF lasts some microseconds and ends at the onset of the submicrosecond-scale fast transition (FT), which signifies the end of BTP. During the BTP, the current rises from the UCL level of the order of tens to hundreds of amperes to about 50% of the overall (SF + FT) current peak, which is of the order of tens of kiloamperes (for negative first strokes). This two orders of magnitude current rise during the BTP occurs before the collision of hot leader channels inside the CSZ; that is, before the onset of return stroke proper.

## 1. Introduction

The lightning attachment process is still one of the most poorly documented lightning processes, although considerable insights into this process have recently been made from observations of natural lightning, as well as from the experiments with rocket-and-wire triggered lightning and long laboratory sparks. This process can be viewed as a transition from the leader stage to the return-stroke stage (e.g., Ref. [7], Ch. 4), which determines the lightning strike point. Therefore, an adequate understanding of the attachment process has important implications for the engineering computational tools widely used in estimating the lightning incidence to different elements of structure to be protected or in identifying the vulnerable parts of the structure, such as the electrogeometrical model, the leader-progression model, and the rolling-sphere method. It is generally assumed that the attachment process in natural lightning consists of two phases: the development of one or more upward leaders (one of which becomes the upward connecting leader (UCL)) extending from grounded objects toward the approaching downward leader (DL) and the so-called breakthrough phase (BTP), which is also known as the final jump. Illustration of the lightning attachment process followed by the return-stroke process is given in Fig. 1. The BTP starts when the poorly-conducting streamer zones developing ahead of the hot channels of negative DL (−SZ) and positive UCL (+SZ) come in contact, and a common streamer zone (CSZ) is formed. Note that the DL is not connected to the grounded object at stage I, and that it first becomes connected to the grounded object via the high-impedance CSZ between stages I and II. It is only between stages II and III that the hot leader channels collide and the CSZ is eliminated (short-circuited by a hot channel). As a result, the low-impedance connection to the grounded object is established. In this

* Corresponding author at: Department of Electrical and Computer Engineering, University of Florida, Gainesville, FL 32611, USA.
E-mail address: rakov@ece.ufl.edu (V.A. Rakov).

https://doi.org/10.1016/j.epsr.2019.03.018
Received 31 October 2018; Received in revised form 15 February 2019; Accepted 19 March 2019

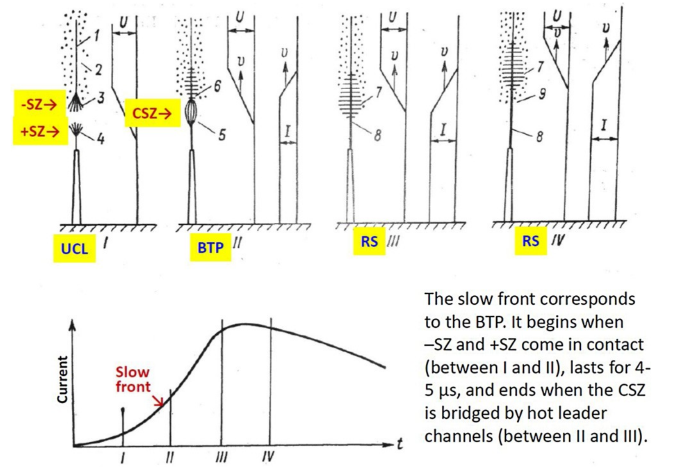


Fig. 1. Schematic representation of the lightning attachment process (stages I and II: upward connecting leader (UCL) and breakthrough phase (BTP), respectively), followed by the return stroke (RS) process (stages III and IV). The corresponding current versus time waveform that would be measured in the strike object is also shown. 1 and 2 — Downward-leader (DL) channel core and its corona sheath, respectively; 3 and 4 — streamer zones of DL (−SZ) and UCL (+SZ), respectively; 5 — common streamer zone (CSZ); 6 — the beginning of reverse corona transferring negative charge from the corona sheath to the channel core; 7 — same as 6, but during the RS process; 8 and 9 — RS channel and residual corona sheath behind the upward-moving RS front, respectively. Adapted from Bazelyan et al. [48].

regard, the shrinking CSZ during the BTP acts as a closing plasma switch whose impedance rapidly reduces with time. It can be also visualized as an equivalent voltage source connected between the hot channels of DL and UCL, which launches two current waves, one moving upward along the DL and the other downward along the UCL. The latter current wave is expected to be reflected at the ground and catch up with the upward-moving current wave to form a single, upward-moving wave, which is traditionally viewed as the return stroke proper.

Many researchers (e.g., Refs. [8–13]) used high-speed cameras to capture video images of UCL in natural lightning terminated on towers or tall buildings, at which UCLs are generally longer. An example of such video record is shown in Fig. 2. In this Figure, one of the branches (barely seen in (a) and (b)) of downward leader (DL) and the upward connecting leader (UCL) are seen to meet tip-to-tip. However, Lu et al. [10] has reported that the DL tip often makes connection to the lateral surface of UCL (also observed in sparks [6], Figs. 6 and 8), while the UCL tip never connects to the lateral surface of DL. Also seen in Fig. 2 (in the left side of frames (a) through (e)) is another upward leader that did not make connection with the DL; it is labeled UUL in (a), which stands for unconnected upward leader. The final lengths of UCL and UUL were estimated to be about 610 m and 360 m, respectively, with the corresponding distances from the camera being 3.3 km and 2.4 km (Weitao Lyu, personal communication, 2018).

UCLs in rocket-triggered lightning were studied by Wang et al. [14], Biagi et al. [15], and Hill et al. [5], with one example (which constitutes the first direct evidence of developing UCL and initially bidirectional RS) being schematically shown in Fig. 3.

Note that no CSZ is seen in Fig. 2, and that CSZ could not be recorded with the photoelectric system, data from which were used in producing the drawing shown in Fig. 3. Tran and Rakov [2,3] estimated the initial length of CSZ for first and new-ground-termination subsequent strokes in natural negative lightning to be 30–40 m or so (see Section 4).

In this paper, recent progress in studying the breakthrough phase (BTP) of the attachment process in lightning and long sparks is reviewed. The main focus is on the new insights gained from recent observations for 3 types of discharges: natural lightning [1–3], rocket-and-wire triggered lightning [4,5], and long sparks [6]. The structure of the paper is as follows. After a brief introduction in Section 1, examples of rare optical images of BTP, including one two-frame record, are presented in Section 2. Section 3 is devoted to a description of signatures of BTP in electromagnetic field records. Interpretation of pulses at the onset of and during the slow front (SF) in field waveforms is also given in Section 3. New synchronized high-speed video and field data acquired at LOG (Lightning Observatory in Gainesville, Florida) are reviewed in Section 4. Characteristics of the attachment process (with emphasis on BTP) in natural lightning, rocket-and-wire triggered lightning, and long laboratory sparks are compared in Section 5. Discussion and summary are found in Sections 6 and 7, respectively.

## 2. Optical images of the breakthrough phase

As noted above, the breakthrough phase (BTP) of the attachment process begins when the streamer zones of DL and UCL come in contact with each other; that is, at the time of establishment of common streamer zone (CSZ). Optical images of CSZ are very rare, particularly for natural lightning. Images of CSZ for rocket-triggered lightning have been presented by Biagi et al. [15] and Hill et al. [5] and by, for example, Lebedev et al. [16], Shcherbakov et al. [17], and Kostinskiy et al. [6] for long laboratory sparks. In all those cases, the CSZ was imaged in a single frame (see an example shown in Fig. 4, left panel), except for the one presented by Kostinskiy et al. [6], who obtained two frames for one event (see Fig. 5).

Kostinskiy et al. [6] presented detailed observations of the connection between positive and negative leaders in meter-scale electric discharges generated by artificial clouds of negatively charged water droplets. One of their records, obtained using a 4Picos framing camera with a built-in image intensifier (optical gain was $5 \times 10^3$), is reproduced in Fig. 5. It is presently the only image of BTP showing the collision of oppositely charged leaders recorded in more than one frame. The distance between the leader tips is about 20 cm in frame (I) and about 4.5 cm in frame (II). Note that only the upward positive leader in (I) is branched, while in (II) both upward positive and downward negative leaders exhibit pronounced branching. In fact, there are two common steamer zones in frame (II) (the single common streamer zone seen in frame (I) is transformed into two common streamer zones in frame (II)). It is likely that two junction points were formed leading to a loop or split in the channel of return-stroke-like process (although no image of the latter is available for this event), a feature that is occasionally seen in both laboratory sparks and lightning. Besides the forked leader channels seen in Fig. 5, multiple connections leading to a loop or split in the channel, can be formed sequentially (probably because the impedance of a single connection is too high), as evidenced by the so-called slow-front pulses discussed in Section 4.

Kostinskiy et al. [6] estimated positive and negative leader speeds inside the common streamer zone for two events. Higher leader speeds were generally associated with higher leader currents. They also reported that the infrared brightness of the junction region (the section of plasma channel that replaced the common streamer zone) was typically a factor of 5 or so higher than for channel sections either below or above that region. The infrared brightness probably represents the gas temperature and, hence, the energy input to the channel.

Single-frame optical images of BTP (CSZ) in rocket-and-wire triggered lightning and in natural lightning are shown in Section 3 (see Fig. 9a, Frame 3) and in Section 4 (see Fig. 10, −1.9-μs frame), respectively. Single-frame images of CSZ in rocket-triggered lightning are also found in Biagi et al. ([15], Fig. 4), in Gamerota et al. ([18], Figs. 1–3), and in Hill et al. ([5], Figs. 2a, 5, and 8; with Fig. 2a being reproduced in Fig. 9a of this paper). Another single-frame image of CSZ in natural lightning is found in Tran and Rakov ([2], Fig. 3a).

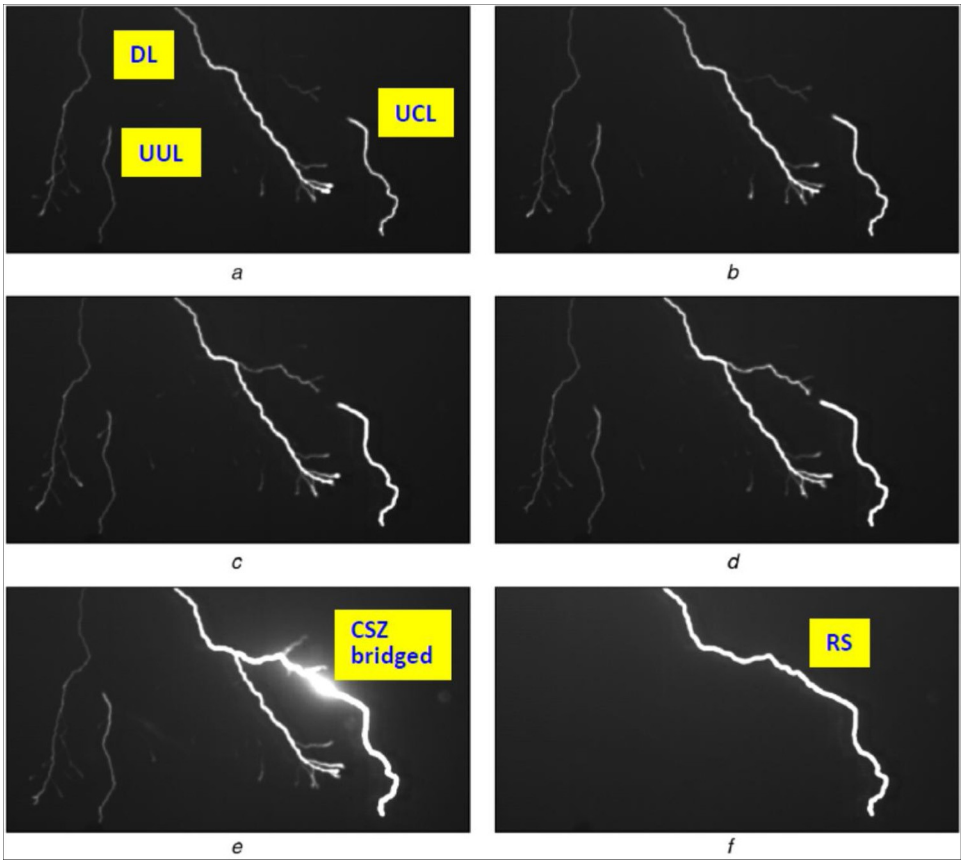


Fig. 2. Six frames of the high-speed video record of the first stroke in flash F1263 captured by Photron FASTCAM SA5 camera with a sampling rate of 50,000 fps (20-μs interframe interval) at TOLOG, China. Frames (a) through (e) are consecutive, and the beginning of exposure of frame (f) is 580 μs after the end of exposure of frame (e). The onset of the return stroke occurred just after the end of the exposure of frame (e), in which the common streamer zone (CSZ) was bridged. Downward leader, upward connecting leader, and unconnected upward leader are labeled in (a) as DL, UCL, and UUL, and return stroke is labeled in (f) as RS. Adapted from Lu et al. ([10], Fig. 3).

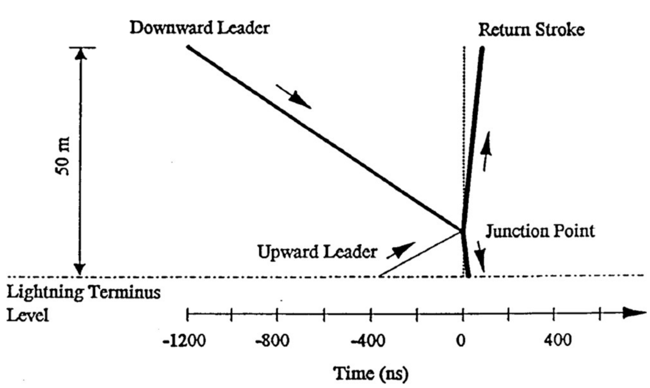


Fig. 3. Schematic representation of negative downward and positive upward leaders meeting at the junction point, about 10 m above the strike-object top, and initially bidirectional return-stroke process in rocket-triggered lightning at Camp Blanding, Florida. The drawing is based on records obtained using a photoelectric system ALPS with 3.6-m spatial and 100-ns time resolution. Adapted from Wang et al. [14].

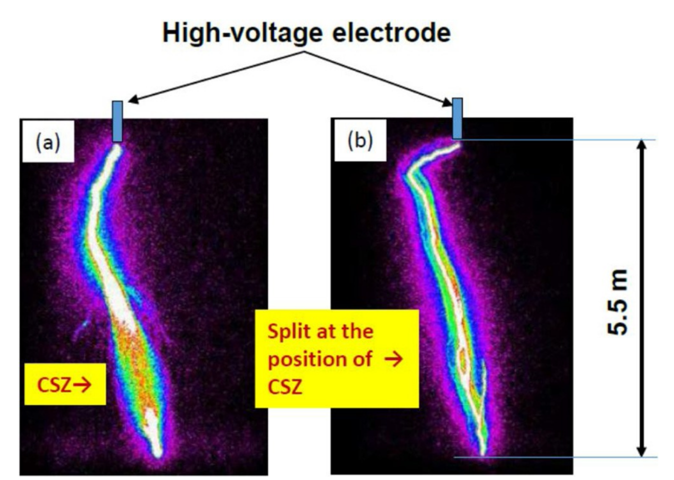


Fig. 4. Single-frame image-converter-camera K008 images of two negative sparks in a 5.5-m gap obtained with a frame exposure of 0.2 μs. The high-voltage electrode was negative. Light intensity is color-coded, with the white color corresponding to saturation. The negative DL, positive UCL, and CSZ are seen in (a), while in (b) the CSZ is already bridged by hot channels of DL and UCL, which connected at the position of split in the lower part of the channel. Adapted from Shcherbakov et al. [17].

## 3. Signatures of the breakthrough phase in lightning electric field records

The initial rising part of return-stroke electric field waveforms can be separated into two phases, as illustrated in Fig. 6. The first one is the so-called "initial slow front" or simply "slow front" (labeled SF in Fig. 6), described by Weidman and Krider [19] as an initial portion or front, which for first strokes rises slowly for 2–8 μs to about half the field peak. The second part, which follows the slow front, is an abrupt transition to peak, typically referred to as the "fast transition" (labeled FT in Fig. 6). The latter, according to Weidman and Krider [19], has a 10-to-90% risetime of 0.2 μs or less for first strokes, when the field propagation is over seawater. The shape of the slow front is typically concave.

Nag et al. [1] reported from two-station electric field measurements that the SF duration at far (46–48 km) distances was similar to that at near (0.51–3.6 km) distances. It has been found from modeling [1,20] that the SF within a few tens of meters of the lightning channel is dominated by the electrostatic field component, at 100 km it is essentially determined by the radiation field component, and at 500 m it is

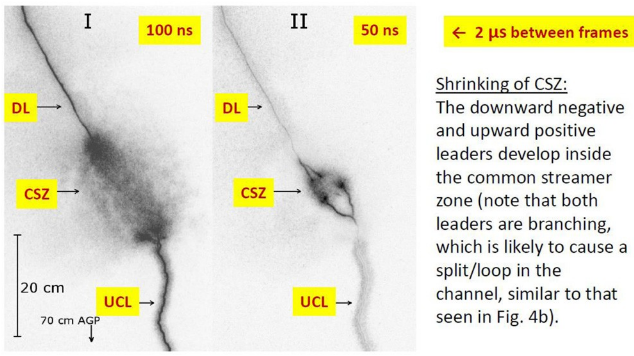


Fig. 5. Two frames obtained with an image-enhancement camera, both showing the CSZ in a negative discharge to ground generated by a cloud of negatively-charged water droplets. The optical gain was 5 × 10 [3]. The exposure time for frame (I) was 100 ns and for frame (II) it was 50 ns. The time interval between frames was 2 μs. Labeled are the electrodeless, negative downward leader (DL), positive upward connecting leader (UCL), and the common streamer zone (CSZ). AGP stands for "above the grounded plane". Adapted from Kostinskiy et al. [6].

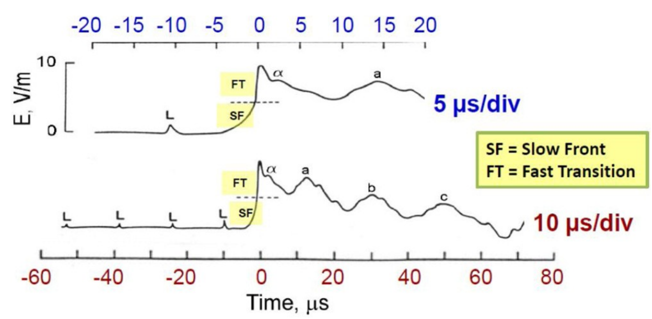


Fig. 6. Electric field waveform of a negative first return stroke shown on two time scales, 5 μs/div and 10 μs/div. The fields are normalized to a distance of 100 km, assuming that the field peak is inversely proportional to distance. Leader step pulses (L), slow front (SF), fast transition (FT), and subsidiary peaks (not discussed in this paper) are indicated. Adapted from Weidman and Krider [19].

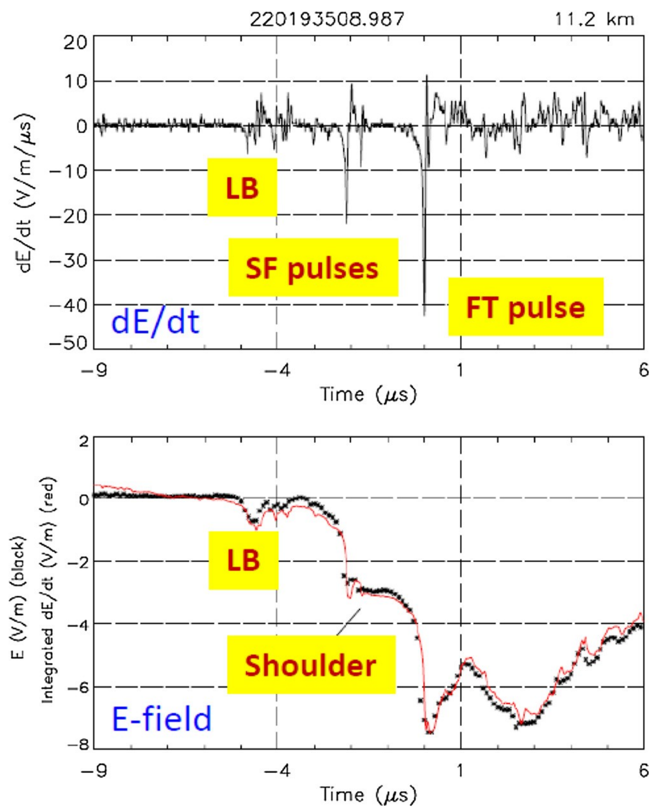


Fig. 7. A negative first return stroke whose dE/dt waveform (top panel) contains additional pulses during the SF (in the −4 μs to −1 μs interval and no additional pulses within ± 1 μs of the dominant peak (FT pulse); such events were labeled Type C by Murray et al. ([23]; they constituted 28% of their dataset). LB stands for "leader burst" (noted to be different from leader step pulses). In the bottom panel, the integrated dE/dt waveform is shown in red, and the small asterisks denote individual samples of electric field waveform obtained with the 10-MHz digitizer. Adapted from Murray et al. ([23], Fig. 11b). (For interpretation of the references to color in this figure caption, the reader is referred to the web version of this article.).

composed of comparable contributions from all three components of electric field.

Jerauld et al. [20] and Nag et al. [1] attributed the slow front (SF) in return-stroke electric field waveforms to the SF in the corresponding channel-base current waveforms. Nag et al. [1] explicitly stated (apparently for the first time) that the mechanism of SF formation in the current is related to the BTP of the attachment process. This means that the SF process begins when the streamer zones of DL and UCL first come in contact and that the following extension (and probably acceleration) of hot leader channels takes place inside the common streamer zone, until their collision which signifies the end of the SF process and the beginning of the FT process.

It is worth noting that apparently the first attempt to relate the slow front to a streamer region initially involved in the descending-leader connection to ground was made by Cooray [21]. He suggested that when the streamer zone of downward negative leader comes in contact with the ground the return-stroke channel (or UCL) will extend upward inside the negative streamer zone. Also, Cooray et al. [22] modeled the slow front in both negative and positive strokes by assuming that UCL extends at an exponentially increasing speed until it makes contact with the hot channel of the descending leader. In both these works, it was assumed that UCL does not start (if at all) until the streamer zone of descending leader touches the ground, which is unlikely, particularly for lightning strikes to object significantly protruding above the surrounding terrain.

In Fig. 6, the SF is smooth, which is not always the case. Fig. 7 shows the electric field waveform of negative first return stroke (bottom panel) and the corresponding dE/dt waveform (top panel), inverted relative to the waveforms shown in Fig. 6, with structured SF. The part of dE/dt records corresponding to SF in electric field records often exhibits superimposed pulses that are labeled "SF pulses". The latter may appear as shoulders in the corresponding electric field records, as seen in the bottom panel. According to Murray et al. [23], only 35% of natural-lightning electric field waveforms exhibit smooth SF and FT, similar to those seen in Fig. 6, and the majority of waveforms show SFs (in dE/dt records) with superimposed pulses.

The beginning of SF is often marked by a sequence of dE/dt pulses (sometimes a single pulse) that is referred to as the "leader pulse burst" or just "leader burst". Such leader burst, labeled LB, is seen in Fig. 7.

Next, we will discuss in more detail, with reference to works of Howard et al. [4] and Hill et al. [5], the interpretation of pulses at the onset of and during the slow front (LB and SF pulses).

Howard et al. [4] studied the sources of dE/dt pulses around the transition from leader to return-stroke stage in 3 natural-lightning first strokes and 1 rocket-triggered-lightning stroke and identified three types of pulses (besides the regular step pulses), which they labeled the leader pulse burst (or just leader burst, LB), SF pulses, and the FT pulse. The LB was defined as a group of dE/dt pulses immediately preceding or at the onset of the SF and the SF pulses as dE/dt pulses occurring during the SF. As the name suggests, the FT pulse is the dominant dE/dt pulse corresponding to the FT part of the return-stroke field waveform.

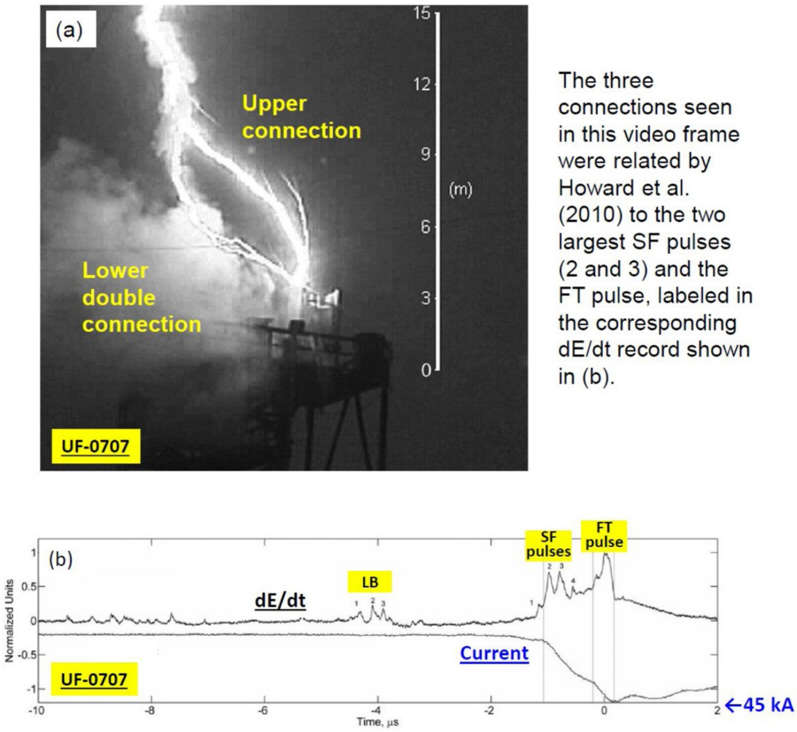


Fig. 8. (a) Single ordinary video frame showing one of the return strokes in triggered-lightning flash UF-0707 with a total of 3 connections (a single upper connection and a double lower connection) between the negative DL and positive UCL. The height scale relative to the launch-tower platform is shown to the right from the lightning image. The longitudinal dimension of the connection region, which probably corresponds to the initial length of CSZ, is about 8 m or so. (b) The corresponding dE/dt waveform (upper trace) and the channel-base current waveform (lower trace). The leader burst (LB), SF pulses, and FT pulse are marked. The current peak was 45 kA. Adapted from Howard et al. [4].

This classification is similar to that previously used by Murray et al. [23]. In contrast with the SF and FT pulses, the sources of LB pulses in Howard et al.'s [4] study exhibited rapid movements and were prolific X-ray producers [X-ray bursts at the time of collision of opposite polarity streamers were predicted by Cooray et al. [24] and observed in laboratory spark experiments [25,26]. Those observations have been followed by a number of modeling efforts [27–31]]. Howard et al.'s [4] electric field and current records for the rocket-triggered-lightning stroke are shown in Fig. 8. They inferred that the FT pulse and the SF pulses were all of the same nature and associated with multiple connections sequentially made between the downward negative and upward positive leaders during the BTP. It is worth noting that besides the 3 successful connections (a single upper connection and a double lower connection) seen in Fig. 8a, there were also attempted connections in the form of unconnected downward negative and upward positive branches extending toward each other near the junction region. Attempted connections are also seen in the right panel of Fig. 9a.

More recently, Hill et al. [5], who imaged the common streamer zone in rocket-triggered lightning strokes (see their Figs. 2a, Frame 3; 5, Frame 5; and 8, Frame 4), showed that the LB (which can be a single pulse) is associated with a fast increase, to typically many hundreds of amperes, in the channel-base current. They attributed that current increase to "the initial interactions of the downward and upward leader streamer zones". Sources of LB pulses were located within or immediately above the connection region between the downward leader and UCL. They also related each of their SF/FT pulses to a fast, kiloampere-scale increase in the channel-base current followed by a decrease in current rate of rise. One of the events examined by Hill et al. [5] is presented in Fig. 9. Note that Hill et al. [5] reported UCLs that were detected in their channel-base current records, but not accompanied by detectable luminosity in the corresponding optical images. Their "dark currents" were up to about 10 A or so. Visacro et al. [12] reported, for natural lightning terminating on a 60-m tower, that sustained UCLs (identified by the onset of exponential-looking current increase) developed only when the steadily-increasing current in the tower exceeded an apparent threshold of 4 A.

## 4. New synchronized high-speed video and field data acquired at LOG

In this section, we will review the results of recent observations of BTP of the attachment process in natural lightning obtained at the Lightning Observatory in Gainesville (LOG), Florida. Synchronized high-speed (124 or 210 kiloframes per second) optical and wideband electromagnetic field records, corresponding to the ground-attachment process in 1 first and 3 new-ground-termination subsequent strokes of negative polarity have been presented by Tran and Rakov [2,3]. The strike objects were apparently trees with heights not exceeding 30 m or so. Optical and field (dB/dt) records, along with the current waveform inferred from the integrated dB/dt record, for one event are shown, as an example, in Figs. 10 and 11, respectively. The images shown in Fig. 10 were obtained at the 240 kfps framing rate (the exposure time was 3.65 µs and the dead time was 1.11 µs) with spatial resolution of 3.4 m per pixel. Some characteristics of the 4 examined events are summarized in Table 1.

The common streamer zone was imaged (for the first time in natural lightning) for 2 out of 4 strokes. For one of them (event 1236), it was 6.7-m long at the end of exposure of the pre-return-stroke frame, 1.9 µs before the return-stroke current peak (see "Connection region" in the −1.9-µs frame in Fig. 10). The initial length of common streamer zone (CSZ) was estimated for 3 events (1106, 1236, and 1239) to be between 30 and 40 m. For 2 events (1106 and 1236), speeds of positive and negative leaders developing toward each other inside the CSZ were found to be between $2.4 \times 10^6$ and $3.7 \times 10^6$ m/s, and for 1 event (1236), opposite polarity leaders were observed to accelerate inside the CSZ (see Table 1).

The current at the end of the breakthrough phase was estimated to be approximately one-half of the overall current peak, as seen for event 1236 in Fig. 11. Thus, about one-half of the current peak traditionally attributed to the return-stroke process is actually associated with two leaders extending toward each other to collision inside the CSZ. Currents were inferred from the integrated magnetic field derivatives measured at LOG (at a distance of 1.8 km for the event presented in Figs. 10 and 11), using the transmission line (TL) model [32]. This

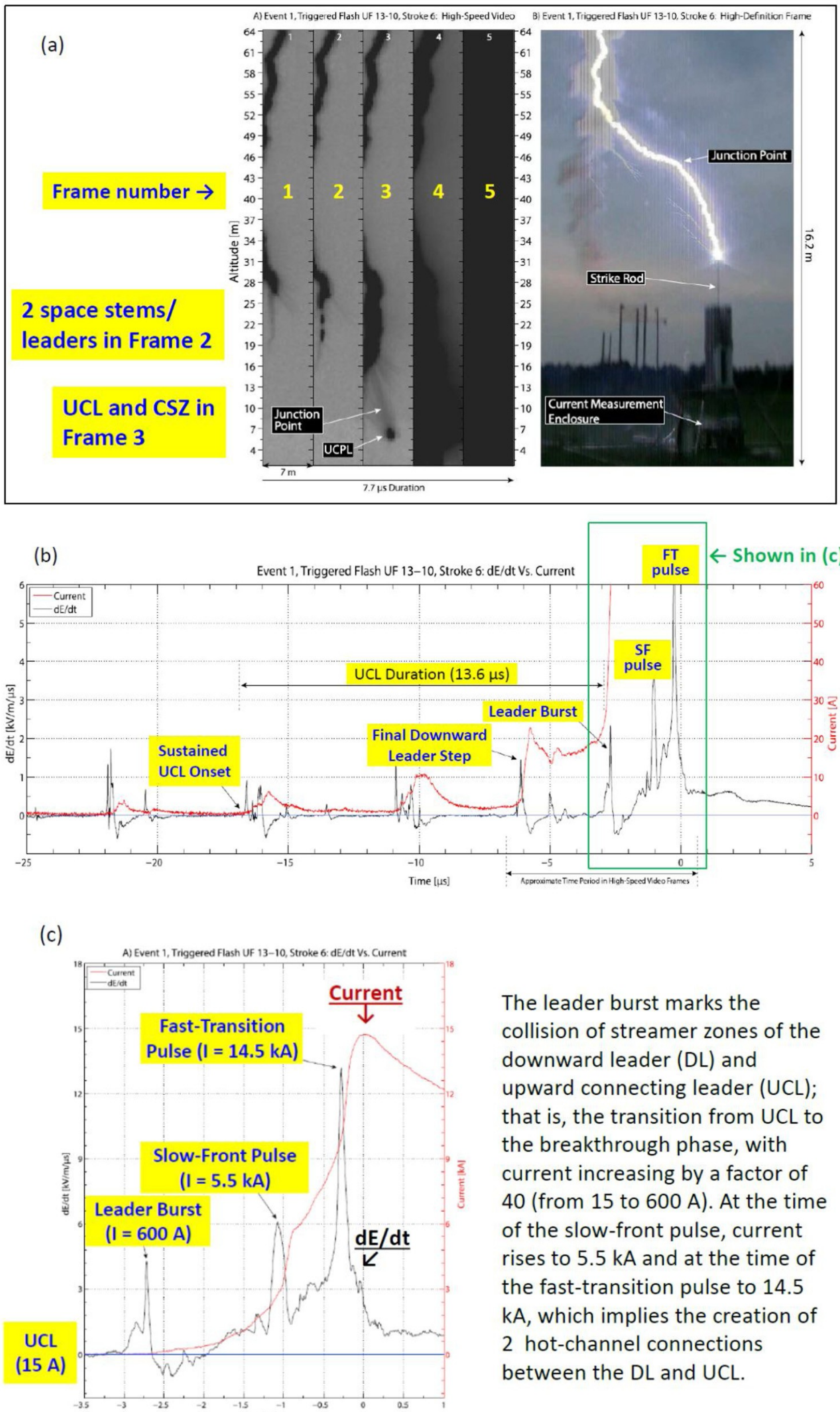


Fig. 9. (a, left panel) Five consecutive 1.54-μs frames (7.7-μs total duration) showing the final downward leader step (Frames 1–3) and the subsequent attachment process (Frames 3–4) for the sixth return stroke of flash UF 13–10 triggered at Camp Blanding, Florida. (a, right panel) Cropped high-definition video frame (30-ms exposure) showing the attachment of the upward and downward leaders at the junction point. Note that the vertical scales in the left and right panels are different by a factor of four. (b) Corresponding dE/dt (black) and channel-base current (red) waveforms shown on a 30-μs time scale. The onset of sustained UCL, final downward leader step, leader burst, SF pulse, and FT pulse are labeled. (c) Same as (b), but shown on a 4.5-μs time scale and with larger dE/dt (18 vs. 6 kV/m/μs) and larger current (18 kA vs. 60 A) scales. Note that Frame 3 in (a) shows a UCL (labeled UCPL, where P stands for positive) and an approximately 10-m long and 5-m wide CSZ. Adapted from Hill et al. [5]. (For interpretation of the references to color in this figure caption, the reader is referred to the web version of this article.).

approach implies that the LB, SF, and FT field signatures (the initial 5 μs or so of the return-stroke field waveform, including the LB and SF) are essentially radiation, which is supported by essentially identical shapes of the electric field and integrated dB/dt (current) fronts. The applicability of the TL model to both SF and FT was demonstrated by Jerauld et al. [20] and Nag et al. [1]. The use of the TL model requires a value of the return-stroke speed, which was not known. In order to avoid this difficulty, the NLDN-reported peak current was assigned to the integrated dB/dt waveform peak, and the rest of the waveform was scaled accordingly. The NLDN here stands for the U.S. National Lightning Detection Network.

The LB current hump peak (Mean = 1.9 kA) was found to be

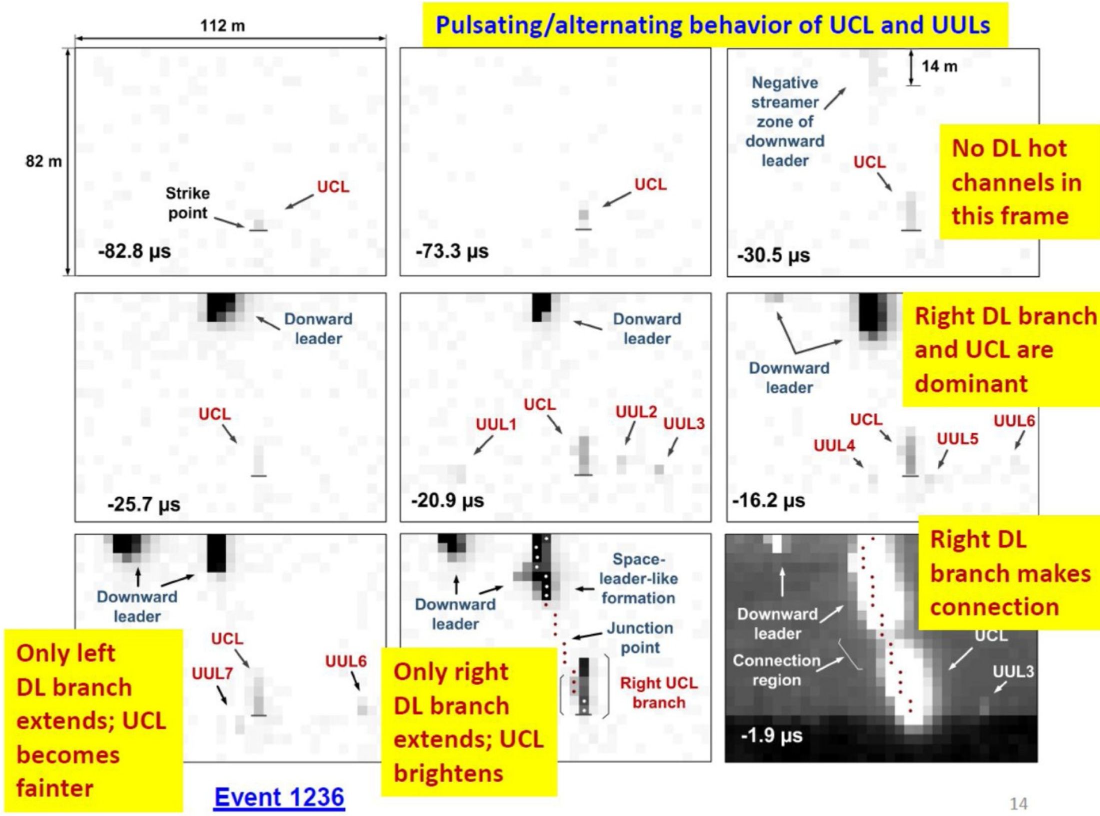


Fig. 10. Illustration of CSZ and pulsating/alternating behavior of UCL and UULs. Shown are 9 selected (not all consecutive) frames of the attachment process in natural negative lightning stroke (event 1236) recorded using a Phantom V310 high-speed framing camera at LOG. The frames show the development of the downward leader (DL), upward connecting leader (UCL), and 7 unconnected upward leaders (UULs). The interframe interval was 4.7 μs, and the spatial resolution was 3.4 m per pixel. A 6.7-m long CSZ (labeled "Connection region") is seen in frame −1.9 μs. All frames are background-luminosity subtracted, inverted, and enhanced with the same level for improved visualization, except for frame −1.9 μs. Adapted from Tran and Rakov [2].

comparable to the expected step current peak of negative leaders near ground. It appears that the LB process differs from the regular leader step in that the negative corona streamer burst of the former makes contact with the positive streamer zone of grounded UCL channel, as further discussed in Section 6. Note that Tran and Rakov [2,3] have defined the BTP duration as the sum of LB and SF durations. The mean LB duration in their study was 1.9 μs and the mean SF duration was 2.8 μs, yielding the mean BTP duration of 4.7 μs.

It is worth noting in Fig. 10 that, besides the UCL, a number of unconnected upward leaders (UULs) occurred in response to the same

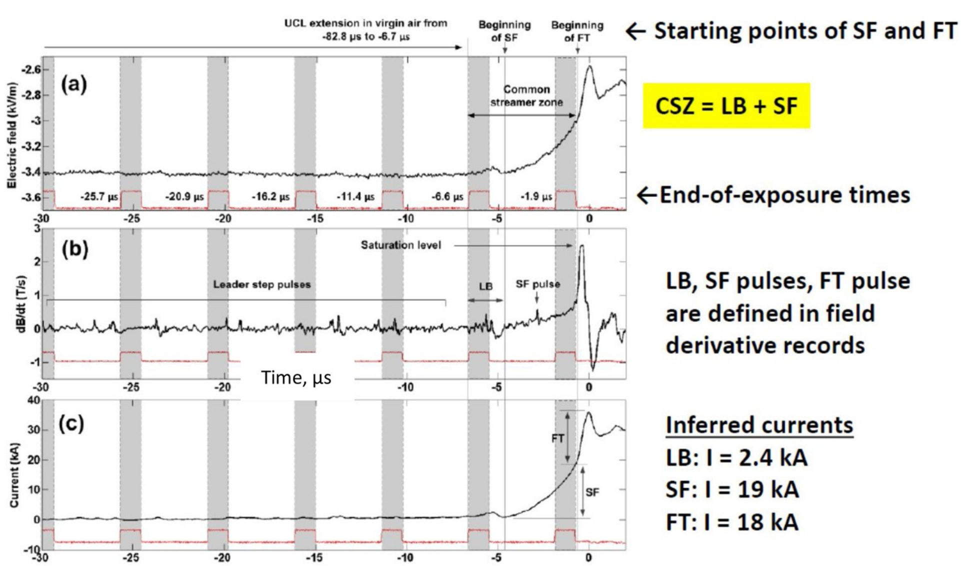


Fig. 11. (a) Electric field, (b) magnetic field derivative (dB/dt), and (c) inferred current for event 1236 whose optical images are presented in Fig. 10. The fields were measured at a distance of 1.8 km. Blank areas correspond to exposure times and shaded areas to dead times of the framing camera, as determined from the Strobe signal (shown in red) of the camera (synchronization accuracy was better than 200 ns). LB, SF, and FT stand for the leader burst, slow front, and fast transition, respectively. The beginning of SF is marked by the beginning of the ramp in dB/dt record and is preceded by the LB. The beginning of FT is the abrupt increase at the end of the SF ramp in dB/dt record. The common streamer zone (CSZ) is assumed to be established at the beginning of LB and completely bridged by the DL and UCL hot channels at the end of SF (the beginning of FT). The end of exposure of frame −1.9 μs occurred after the SF pulse (marked in (b)), but before the end of SF; that is, during the breakthrough phase. Adapted from Tran and Rakov [2]. (For interpretation of the references to color in this figure caption, the reader is referred to the web version of this article.).

Table 1
2D speeds of downward negative leaders and UCLs, initial length of common streamer zone, and BTP current for the 4 events studied by Tran and Rakov [2,3].

| Event ID | Height of downward leader tip at the initiation of UCL (m) | Height of downward leader tip at the onset of common streamer zone (m) | Speed in virgin air ($10^5$ m/s) | | | Initial length of streamer zone (m) | Speed in common streamer zone ($10^6$ m/s) | | | Speed immediately prior to FT[c] ($10^6$ m/s) | Current at the end of pre-FT frame (kA) |
|---|---|---|---|---|---|---|---|---|---|---|---|
| | | | Downward leader | UCL | Speed ratio DL/UCL | | Downward leader | UCL | Speed ratio DL/UCL | | |
| 1106 | 59[a] | 46 | 9.1 | - | - | 40 | 3.7 | 2.4 | 1.5 | - | 23 |
| 1236 | >64 | 42 | 7.2 | 1.8 | 4.1 | 29 | 2.5 | 2.5 | 1.0 | 3.2 | 9.9 |
| 1238 | 19 | - | 2.8 | 6.0 | 0.5 | - | - | - | - | - | 2.5 |
| 1239 | 69 | 44 | 7.7 | 2.6 | 3.0 | 29 | - | - | - | 3.8 | - |
| Mean | >53[b] | 44 | 6.7 | 3.4 | 2.5 | 33 | 3.1 | 2.5 | 1.3 | 3.5 | 12 |
| Sample size | 4 | 3 | 4 | 3 | 3 | 3 | 2 | 2 | 2 | 2 | 3 |

[a] Assuming that the UCL was initiated at the end of exposure of frame -8.8 μs.
[b] Median = 62 m.
[c] Speeds of UCL and downward leader are assumed to be equal to each other.

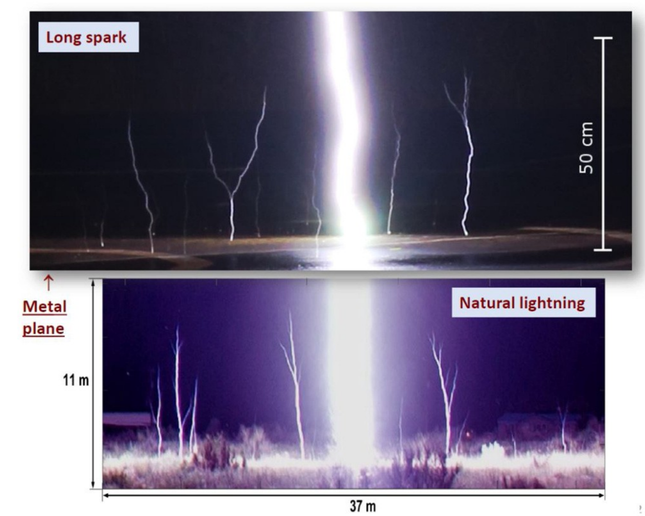


Fig. 12. (top) Still photograph of multiple upward unconnected leaders (UULs) near the main spark channel (in the center) observed at the High-Voltage Research Center at Istra, Russia. The spark was produced in a 4.5-m rod-plane gap, with the polarity of high-voltage electrode (rod) being negative. Courtesy of V.S. Syssoev and A.Yu. Kostinskiy. (bottom) Still photograph of multiple UULs near the main lightning channel (in the center) observed in New Mexico. Exposure time was about 10 s and the spatial resolution was 5.5 cm per pixel. Distance to the main channel was 460 m. A total of 12 UULs (probably not simultaneous) are seen, 6 of which are branched. The mean UUL length was 4.1 m and mean distance to the strike point was 8.8 m. Adapted from Cummins et al. [49].

DL. Many better-resolved images of multiple UULs (mostly still photographs) can be found in the literature. They have been documented to originate from the ground, trees, water surface, and even from metallic plane electrodes (in long laboratory sparks). Examples of multiple UULs from a metallic plane (in a laboratory spark) and from relatively flat ground (in natural lightning) are shown in the top and bottom panels of Fig. 12, respectively. Fig. 12 (bottom panel) shows only one of the two strokes of the two-stroke lightning flash captured by the camera, the other one being outside the cropped image shown in Fig. 12 (bottom). Interestingly, the other stroke, whose channel terminated on ground about 300 m away from the one seen in Fig. 12 (bottom), showed no optically detectable UULs.

Note also that the majority of UCLs and UULs reported by Tran and Rakov [2,3] exhibited a pulsating behavior (brightening/fading cycles) in response to the approaching branches of DL, as seen in Fig. 10. In one case (event 1239), the UCL was preceded by a UUL (see Fig. S1 of Ref. [3]), which means that the initiation of upward leader does not necessarily determine the strike point, as assumed by, for example, Golde [33]. Indeed, an upward leader may fail to intercept the downward leader and another, later initiated upward leader may become the UCL. In this regard, it is probably reasonable to assume that the strike point is uniquely determined only at the time of establishment of CSZ, as done by Rakov and Lutz [34] and Cooray et al. [35].

## 5. Comparison of the attachment process in natural lightning, rocket-triggered lightning, and long laboratory sparks

Comparison of the characteristics of attachment process (with emphasis on BTP) in natural lightning, in rocket-triggered lightning, and in long laboratory sparks produced by small artificially charged clouds is presented in Table 2. The primary difference between rocket-triggered lightning and natural lightning, when the attachment process is concerned, is the availability of a previously-conditioned (warm-air) path to the strike point, which facilitates the occurrence of lower-peak-current strokes in rocket-triggered lightning and is absent in new-ground-termination strokes in natural lightning. Laboratory sparks develop in virgin air, similar to new-ground-termination strokes in natural lightning, but occur on much smaller spatial scales. The significant differences between lightning and laboratory sparks (at least those produced by small artificially charged clouds) and between first and subsequent lightning strokes in terms of the electric potential, gap length, or charge transfer are not likely to qualitatively influence the physical processes in the CSZ. Indeed, according to Kostinskiy et al. [6], the discharge processes in the streamer zone of a leader in virgin air are determined by the electric field produced by the charges of leader tip, charges on a short segment of leader channel (including its corona sheath) just behind the tip, and charges of streamers forming the streamer zone; they only weakly depend on the large-scale external electric field produced by charges in the cloud, on leader branches (if any), etc. During the BTP, the electric field intensity inside the CSZ increases, as the two oppositely-charged hot leader channels approach each other, and the influence of the external field on the processes there becomes even less significant. On the other hand, caution is to be exercised in interpreting the results for laboratory sparks produced by impulse generators, since the processes during the BTP may be significantly influenced by the impulse-generator circuitry (in particular, by the presence and value of series resistor in the generator circuit). According to Larsson [36], the duration of BTP (final jump) without a series (braking) resistor in the generator circuit is a few microseconds, and with a 1-MΩ series resistor it increases to 55 ± 7 μs.

Table 2
Characteristics of the attachment process in natural lightning strokes [2,3] vs. those in rocket-triggered lightning strokes [5] and in long spark discharges produced by artificial clouds of negatively charged water droplets [6]. Adapted from Tran and Rakov [2].

| Parameter | Natural lightning (Tran and Rakov, 2017) | | | | Rocket-triggered lightning (Hill et al., 2016) | | | | Discharges produced by artificial clouds (Kostinskiy et al., 2016) | |
|---|---|---|---|---|---|---|---|---|---|---|
| | Min | Max | AM | Sample size | Min | Max | AM | Sample size | Event 1 (their Figs. 1 and 2) | Event 2 (their Figs. 3 and 4) |
| Maximum UCL extent, m | 11 | 25 | 18 | 4 | 3.5 | 11.0 | 6.9 | 3 | ~1 | ~1 |
| UCL duration, us | 21 | 76 | 42 | 3 | 5.0 | 21 | 11 | 51 | > 30 | ~50 |
| BTP duration, us | 3.3 | 6.0 | 4.7 | 4 | 0.8 | 4.6 | 1.8 | 51 | 2.0 | 2.4 |
| Initial common streamer zone length, m | 29 | 40 | 33 | 3 | ~6 | ~10 | ~8 | 2 | >0.17 | >0.2 |
| Current at the end of SF (BTP), kA | 3.6 | 24 | 16 | 4 | 3.6 | 7.8 | 6.2 | 3 | 4.9 A | 4 A |
| Return-stroke peak current, kA | 7.7 | 55 | 34 | 4 | 12 | 15 | 14 | 3 | > 8 A | > 8 A |
| End-of-SF current relative to peak current, % | 43 | 52 | 48 | 4 | 32 | 53 | 46 | 3 | <71 | <50 |

In general, parameters for natural lightning in Table 2 are 2–4 times greater than their counterparts for rocket-triggered lightning. Arithmetic means of maximum UCL extent and BTP duration for rocket-triggered lightning are a factor 2–3 smaller than for natural lightning, while for the UCL duration and initial length of CSZ the difference is about a factor of 4. Interestingly, the BTP duration for long sparks is similar to that for rocket-triggered lightning. The final BTP (pre-FT) current in rocket-triggered lightning is a factor of 2–3 lower than in natural lightning, which is similar to the difference between the overall peak currents.

It appears from the comparison of the results for natural lightning with those for triggered lightning and for long laboratory sparks, along with other observations reviewed in this paper, that in each case the attachment process involves a UCL, formation of CSZ between the hot channels of DL and UCL, and the bridging of CSZ by colliding hot leader channels. Based on that comparison, Kostinskiy et al. [6] inferred that phenomenologically the attachment process of all three types of electric discharges represented in Table 2 is essentially the same.

We now discuss the differences between the negative streamer zones of stepped leaders developing in undisturbed air and dart-stepped leaders following a previously formed, but decayed channel to ground. In the latter case, the channel is usually not luminous, but its temperature, about 3000 K, is still elevated relative to ambient, with the corresponding air density being about a factor of 10 lower than ambient.

Gamerota et al. [18] examined in detail negative corona streamer bursts in three dart-stepped leaders in rocket-triggered lightning, which they referred to as “guided corona”, since it extended primarily along the remnants of preexisting channel. They also considered the so-called “side-corona” streamers that appeared to extend sideways from the leader channel (into the ambient air). The mean length of “guided corona” was 9 m, while the maximum measurable length of “side-corona” streamers ranged from 2 to 6 m with a mean of 4 m. The lengths of imaged CSZs for the same three rocket-triggered lightning strokes were 7, 14, and 16 m (the corresponding return-stroke peak currents were 12, 22, and 17 kA) with a mean of about 12 m. Thus, it appears that the CSZ was mostly composed of negative streamers. No positive streamer zone of UCL was optically detected in that study, even though the settings of the camera were optimized for recording low-luminosity phenomena. It is possible that the negative streamers from the tip of descending leader developed in part along the path of optically undetectable positive streamers from the UCL tip. [Positive streamers require about a factor of 2 lower electric field for their propagation than negative streamers.] Gamerota et al. [18] found that the negative corona streamer burst was formed in a time shorter than the interframe interval of 1.54 μs, which is consistent with < 1-μs formation times of negative corona streamer bursts in long sparks inferred by Kostinskiy et al. [37]. In contrast with triggered-lightning streamer bursts, the long-spark corona streamer bursts developed in virgin air and emanated from the newly-formed leader tip in essentially all directions (exhibiting nearly spherical appearance).

Petersen and Beasley et al. [51] presented streamer zones of a negative stepped leader, developing in undisturbed air, and a negative dart-stepped leader, developing along a preexisting, but decayed channel, both occurring in the same cloud-to-ground flash at an interval of 43 ms. The NLDN-reported peak current for the first stroke was 35 kA. The streamer zone of the stepped leader fanned out 10–20 m ahead of the tip of each branch. In contrast, the streamer zone of the dart-stepped leader was of “guided” type (with no evidence of “side corona”) and extended over 40 m or so ahead of its tip, along the remnants of preexisting channel, although it might have been influenced by the parasitic light sensitivity (PLS) of the camera.

Only stepped and dart-stepped leaders were discussed above; we are not aware of any optical images of the streamer zone of dart leaders that do not exhibit optical steps. It is possible that the dart-leader streamer zone is significantly influenced by the conduction current induced ahead of the leader tip in the pre-dart-leader channel, whose conductivity is expected to be about 0.02 S/m (similar to the conductivity of clay). In any event, there should be some transitional zone between the channel ahead of the dart-leader front (about 0.02 S/m) and the channel behind the dart-leader front (of the order of $10^4$ S/m) that would play the role of buffer at the time of connection of the dart-leader hot channel to the ground and return-stroke onset.

## 6. Discussion

As noted in Section 1, the occurrence of SF is associated with the operation (closing) of plasma switch whose initial state is the high-impedance CSZ and whose final state is a low-impedance bridge composed of one or more interconnected hot channels. It can be also visualized as an equivalent voltage source connected between the hot channels of DL and UCL, which in effect launches two current waves, one moving upward along the DL and the other downward along the UCL. The hot channels of DL and UCL continue their extension toward each other inside the CSZ. Therefore, the SF part of current and field waveforms, which is commonly attributed to the return-stroke process, is actually associated with the continued extension of the hot channels of two leaders until their collision at the time of FT onset. The SF pulses likely correspond to attempted hot-channel collisions and/or relatively weak connections between the hot channels of DL and UCL. It appears that the BTP process is fundamental to both long sparks and lightning, because their hot leader channels cannot come in contact directly due to the existence of streamer zones at the tips of those hot channels and that SF is a signature of this process in current and field records.

The duration of SF (or LB + SF) should be a measure of the spatial extent of CSZ. It is reasonable to assume that the CSZ is the largest for first strokes (because of their higher intensity and more pronounced corona streamer burst, compared to subsequent strokes) and the smallest for subsequent strokes initiated by dart leaders (whose streamer zone does not include the high-intensity corona streamer burst associated with the step formation process), with subsequent strokes initiated by dart-stepped leaders occupying an intermediate position. Based on this assumption, one should expect the SF duration to progressively decrease from first strokes to subsequent strokes initiated by dart-stepped leaders to subsequent strokes initiated by dart leaders, which is indeed the case: Weidman and Krider [19] reported the mean SF durations in distant natural lightning electric field waveforms for those three types of strokes to be 4.1 μs, 2.1 μs, and 0.9 μs, respectively. Note that the SF durations observed by Weidman and Krider [19] for first strokes (4.1 μs) and subsequent strokes initiated by dart-stepped leaders (2.1 μs) are very close to the corresponding BTP durations (see Table 2) reported by Tran and Rakov [2,3] (4.7 μs) and Hill et al. [5] (1.8 μs), respectively. [Note that the BTP duration is the sum of LB and SF durations and that the LB duration might have been included by Weidman and Krider [19] in their SF duration.] Interestingly, Nag and Rakov [38] reported that the SF duration for positive first strokes in Florida was 6.1 μs, roughly 50% larger than for negative first strokes.

Current during the BTP is of the order of kiloamperes and can reach tens of kiloamperes before the onset of FT, as inferred by Tran and Rakov [2,3]. An example of directly measured current waveform, in which current at the end of BTP (just prior to FT) exceeds 30 kA, is shown in Fig. 13. The kiloampere-scale BTP current is considerably higher than the current associated with UCL, which is of the order of tens to hundreds of amperes. The question is if the pair of converging leaders during the BTP can be viewed (modeled) as a pair of return-stroke waves diverging from an assumed junction point between the DL and UCL. The answer is probably yes, as was demonstrated by Jerauld et al. [20], who successfully reproduced the SF in field-derivative waveforms measured at 15 and 30 m and in the expected electric field waveform at 100 km, using a two-wave transmission-line (TL) model. Also, Nag et al. [1] reproduced the expected electric field waveforms at 500 m and 100 km using two- and three-wave (including reflection from ground) TL models. The results for larger distances are not surprising because the growth of the two leaders into the CSZ is accompanied by the launching of rising-current disturbances along the hot channels above and below the shrinking CSZ, which are largely responsible for the production of distant field waveforms. Indeed, the size of CSZ is small (a few tens of meters and shrinking) compared to the

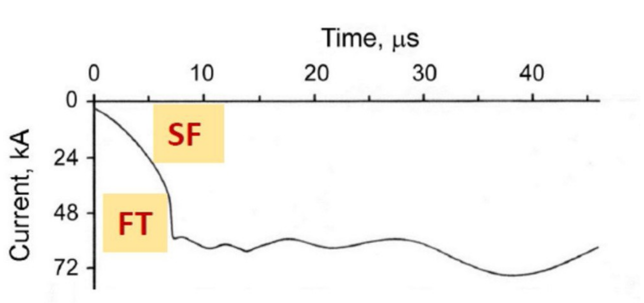


Fig. 13. The waveform of current measured at the bottom of 60-m tower for the first stroke in a negative flash in South Africa. Note the characteristic concave front which appears as a slow front (SF) followed by a fast transition (FT). The duration of SF corresponds to that of the BTP of lightning attachment process. Note that the current magnitude at the end of SF (just prior to FT) exceeds 30 kA, which is greater than 50% of the overall initial current peak. Adapted from Eriksson [50].

length of radiating hot channels, at least of the one above the CSZ, which should be some hundreds of meters by the time of FT onset. Also, the wave propagation speeds along the hot channels (of the order of $10^7$–$10^8$ m/s) are 1–2 orders of magnitude higher than the leader speeds inside the CSZ (of the order of $10^6$ m/s), and a higher speed will lead to a larger radiation field component, which is dominant at larger distances (even during SF; Nag et al. [1]).

On the other hand, the reason for a good agreement between the measured and TL-model-predicted SFs in very close (15 and 30 m) field-derivative waveforms is not so clear and deserves additional discussion. Jerauld et al.'s [20] event was an unusual triggered-lightning stroke whose current waveform exhibited a rise to 20 kA in 2.2 μs (SF) followed by an additional rise from 20 kA to 27 kA in 0.2 μs (FT). The bottom part of its channel had a split suggesting the presence of UCL and multiple hot channel connections formed during the BTP, with the vertical dimension of the split, which probably corresponds to the initial length of CSZ, being about 5 m or so. Jerauld et al. [20] assumed the height of the junction point from which a pair of upward- and downward-moving waves was launched to be 6.5 m (including the 4.5-m height of the strike object). Interestingly, the measured SFs were reproduced not only in the absence of shrinking CSZ, but also when the UCL, strike object, and downward-moving wave were completely neglected in a one-wave TL model, also used by Jerauld et al. [20]. One possible explanation is related to the fact that SFs in dE/dt waveforms at 15 and 30 m are dominated by the electrostatic field component, with the largest contributions to those waveforms coming from sources located in a relatively narrow range of heights. Indeed, according to Rubinstein et al. [39], at 30 m the maximum contribution comes from a height of about 21 m and there are rapidly decreasing contributions from higher and more so from lower heights (assuming that the line charge density is uniform). At 15 m, the maximum contribution comes from about 11 m and the range of heights from which contributions are significant is narrower than at 30 m. Thus, at both 15 and 30 m the "maximum-visibility" heights are above the CSZ, so that the field contributions from the wave propagating upward above the CSZ are likely to be dominant. Some support to this speculation comes from the modeling results of Jerauld et al. [20], who found that a good match to measurements could be achieved only when the wave speed was assumed to be of the order of $10^8$ m/s, which is 2 orders of magnitude higher than the speed characteristic of leaders developing inside the CSZ.

In many lightning protection studies, only the current directly injected into the object is considered and the electromagnetic coupling between the lightning channel and that object is neglected. In such applications, the mechanism of formation of SF in current waveform is immaterial, because the shrinking CSZ is just part of the source.

We now compare steps of the negative stepped leader, produced via connection of a bidirectional space leader to the primary negative leader channel, and pulsations often exhibited by the positive UCL (see Fig. 9b, where one of UCL pulses is labeled "Final Downward Leader Step"). Such UCL pulses are apparently induced by the approaching negative stepped leader (e.g., [5,12]). From measurements of electric field pulses radiated by negative leader steps, Krider et al. [40] inferred that the peak step current is at least 2–8 kA close to the ground, and the minimum charge involved in the formation of a step is 1 to 4 mC. These current and charge values are similar to the estimates made from two-station measurements of close electric and magnetic fields by Rakov et al. [41] for steps of a negative dart-stepped leader in rocket-and-wire triggered lightning. In contrast, the apparently induced current pulses associated with positive UCLs were observed to have peaks of a few tens of amperes for natural-lightning strikes to a 60-m tower [12] and up to 10 A or so for rocket-and-wire triggered lightning [5].

In the absence of approaching negative stepped leader, positive leaders in lightning and long sparks are often assumed to extend continuously (without steps). However, abrupt elongation of positive leader channel in long sparks (in the absence of negative leader) has been well documented in a number of studies (see Kostinskiy et al. [37] and references therein). The stepwise development of positive leader in sparks becomes more pronounced at higher absolute humidity (> 10 g/$m^3$ or so) and longer applied-voltage front (around 1 ms or more). Further, VHF imaging of lightning channels at the time of intermittent propagation of upward positive leaders in rocket-and-wire triggered lightning (e.g., Ref. [42]) does not reveal the presence of in-cloud negative leader, even though negative leaders are known to emit stronger at VHF than positive ones. Thus, positive leaders can definitely propagate in a stepwise manner (elongate abruptly) when the rate of energy supply to the leader tip is insufficient for continuous extension or when the high absolute humidity significantly reduces the effective ionization rate via capture and retention of electrons by water molecules. On the other hand, the mechanism of stepping in positive leaders is likely to be different from that in negative leaders. Indeed, the distinctive feature of negative-leader steps is the space leader that originates from the space stem ahead of the primary leader tip, extends bidirectionally, and eventually makes connection to the primary channel, and the space stems/leaders have never been observed in positive leaders (except for one questionable case presented and discussed by Kostinskiy et al. ([37], Fig. 10).

It is likely that CSZ is established during the LB process, which differs from the regular leader step in that the negative corona streamer burst of the former makes contact with the positive streamer zone of grounded UCL channel, rather than ending in midair. In this view, the LB process serves to connect the hot channel of DL to the ground via a relatively-high-impedance CSZ (neglecting the impedance of the hot channel of UCL). In the negative leader step-formation process (prior to LB), rapid transfer of the primary-leader electric potential to the newly-formed leader tip and the associated corona streamer burst should intensify the positive streamer zone of UCL and lead to the induced UCL stepping discussed above. Such UPL intensification is likely to contribute to the transitioning of negative-leader step to LB. Evidence of intensification of upward positive leaders in response to approaching negative leader branches is seen in Fig. 10.

It is not clear if the extension of negative lightning leader inside the CSZ would involve stepping. An optical image presented by Biagi et al. ([15], Fig. 4) shows evidence of space stem/leader inside the 12-m long CSZ of negative triggered-lightning stroke, whose leader was dart-stepped. Another image is found in Gamerota et al. ([18], Fig. 3); it shows two space stems/leaders located “in series” inside the 7-m long CSZ. Further, the conditions inside the CSZ appear to be conducive to enhanced branching (see Fig. 5). It is also conceivable, as discussed by Kostinskiy et al. [6], that the transformation of CSZ into a hot channel is a complex process that involves competition between the creation and decay of multiple links and possibly floating channel segments inside the CSZ. This competition is possibly influenced by the streamer space charge serving to reduce the electric field near the hot leader channel from which the streamers originate. A sequence of breakdowns may be involved in the bridging of CSZ. Indeed, if, after the initial connection, the impedance of the connection region and the resultant voltage drop remain sufficiently high, an additional breakdown across that region may create an additional connection, in parallel with the initial one. It is worth noting that Gorin and Shkilev [43], who studied positive leaders developing in gaps ranging from 2 to 15 m, observed leader steps inside the streamer zone that emanated from the leader tip and was in contact with the opposite electrode; that is, during the breakthrough phase. The steps were characterized by 10–60-cm lengths and 20–100-A currents. Gorin and Shkilev [43] specifically noted that those steps were influenced by gap length and generator circuitry (the braking resistance).

During the BTP, the current rises from the UCL level of the order of tens to hundreds of amperes to about 50% of the overall (SF + FT) current peak, which is of the order of tens of kiloamperes (for negative first strokes). This two orders of magnitude current rise during the BTP occurs before the collision of hot leader channels inside the CSZ; that is, before the onset of return stroke proper. In the example for rocket-triggered lightning shown in Fig. 9, the current increased from the UCL level of 15 A to 600 A at the time of CSZ onset. It is of interest to estimate, at least roughly, the initial electric conductivity and impedance (resistance) of CSZ. This can be done, using Ohm’s Law, if we use the measured current (600 A) and the observed dimensions of CSZ, estimated using Frame 3 in Fig. 9a (the length is about 10 m and the transverse dimension, roughly corresponding to the diameter, is about 5 m), and make a reasonable assumption on the longitudinal electric field in the CSZ. According to Gorin [44], the average electric field E along the CSZ of several meters in length in negative long sparks is 0.6–1.0 MV/m. If we take E = 1.0 MV/m and assume that the CSZ is roughly a cylinder of a 2.5-m radius, so that its cross-sectional area A is about 20 $m^2$, the electric conductivity σ for current I = 600 A will be $I/(A \times E) = 3 \times 10^{-5}$ S/m. The corresponding dc resistance of 10-m long CSZ is 17 kΩ, which is about an order of magnitude lower than the expected resistance of 10-m long section of pre-dart-leader channel having a radius of 3 cm and conductivity of 0.02 S/m [45]. Our value of conductivity is close to that ($2 \times 10^{-5}$ S/m) estimated by Bogatov et al. [46] for the streamer zone of positive leader in long sparks during the breakthrough phase. It is also not too far from the conductivity estimated by Maslowski and Rakov [47] for the negative corona sheath during the return-stroke process. Our estimate of the initial resistance of CSZ (corresponding to the 600-A current level) can be also compared to the expected resistance of 10-m section of the leader channel, which is 10 m × 3.5 Ω/m = 35 Ω. The corresponding resistance for the return-stroke channel is 0.35 Ω. Note that, according to Rakov [45], the leader and return-stroke channels have each the conductivity of the order of $10^4$ S/m (vs. $3 \times 10^{-5}$ S/m for the CSZ), and their expected channel radii are 0.3 and 3 cm, respectively (vs. 2.5 m for the CSZ). Also, recall that during the BTP the CSZ, which is initially a more or less homogeneous streamer formation, shrinks and is being transformed into one or more hot-channel connections that become part of the return-stroke channel. For this reason, a reasonable estimate of conductivity and resistance of CSZ is only possible at its initial stage, when it is a more or less homogeneous streamer formation.

## 7. Summary

The current understanding of the breakthrough phase (BTP) of lightning and long-spark attachment process can be summarized as follows.

1 The BTP (also known as the final jump) starts when the poorly-conducting streamer zones, developing ahead of the hot channels of negative downward leader (DL) and positive upward connecting leader (UCL), come in contact and a common streamer zone (CSZ) is formed. The beginning of BTP (establishment of CSZ) is usually marked by an abrupt current rise, a burst of dE/dt pulses (leader burst or LB), and hard X-ray emission.
2 It is likely that the LB process differs from the regular leader step only in that the negative corona streamer burst of the former makes contact with the positive streamer zone of grounded UCL channel, rather than ending in midair. In this view, the LB process serves to connect the hot channel of DL to the ground via a relatively-high-impedance CSZ (neglecting the impedance of the hot channel of UCL). In the negative leader step-formation process (prior to LB), rapid transfer of the primary-leader electric potential to the newly-formed leader tip and the associated corona streamer burst should intensify the positive streamer zone of UCL and lead to the abrupt extension of UCL channel (its induced stepping). Such UPL intensification is likely to contribute to the transitioning of negative-leader step to LB.
3 During the BTP, hot channels of both DL and UCL extend toward each other inside the CSZ, resulting in its shrinking, until the high-impedance CSZ is eliminated and a low-impedance connection of

the negative leader to the grounded object is established. The process of bridging the CSZ by one or more hot leader channels is accompanied by the formation of slow front (SF) in the channel current and in electric and magnetic field waveforms at both close and far distances from the channel. The SF lasts some microseconds and ends at the onset of the submicrosecond-scale fast transition (FT), which signifies the end of BTP. [Note that the BTP duration is the sum of LB and SF durations.]

4 The shrinking CSZ during the BTP acts as a closing plasma switch whose impedance rapidly reduces with time. The switch is connected between the hot channels of DL and UCL at the beginning of BTP; its initial state is the high-impedance (of the order of 20 kΩ or so) CSZ and its final state is a low-impedance bridge composed of one or more interconnected hot channels. It can be also viewed as a voltage source which in effect launches two current waves, one moving upward along the DL and the other downward along the UCL.

5 During the BTP, the current rises from the UCL level of the order of tens to hundreds of amperes to about 50% of the overall (SF + FT) current peak, which is of the order of tens of kiloamperes (for negative first strokes). This two orders of magnitude current rise during the BTP occurs before the collision of hot leader channels inside the CSZ; that is, before the onset of return stroke proper.

6 It appears that in computing lightning return-stroke electromagnetic fields the pair of converging leaders during the BTP can be modeled as a pair of return-stroke waves with SFs that are diverging from an assumed junction point between the DL and UCL. This is the case because the growth of two leaders into the CSZ is accompanied by the launching of rising-current disturbances along the hot channels above and below the shrinking CSZ, these rapidly moving disturbances (particularly the upward moving one) being largely responsible for the production of relatively distant field waveforms. Even at very close distances the contribution from leader channels extending inside the CSZ seems to be small.

7 Arithmetic means of maximum UCL extent and BTP duration for rocket-triggered lightning are a factor of 2–3 smaller than for natural lightning, while for the UCL duration and initial length of CSZ the difference is about a factor of 4. The final BTP (pre-FT) current in rocket-triggered lightning is a factor of 2–3 lower than in natural lightning, which is similar to the difference between the overall peak currents. BTP duration in long sparks is similar to that in rocket-triggered lightning. It appears that the BTP process is fundamental to both long sparks and lightning, because their hot leader channels cannot come in contact directly due to the existence of streamer zones at their tips.

8 For the CSZ seen in Fig. 9a (Frame 3), if we take the longitudinal electric field E = 1.0 MV/m and assume that the CSZ is roughly a cylinder of a 2.5-m radius, so that its cross-sectional area A is about 20 $m^2$, the electric conductivity σ for current I = 600 A will be $I/(A \times E) = 3 \times 10^{-5}$ S/m. The corresponding dc resistance of CSZ, whose length is about 10 m, is 17 kΩ, which is about an order of magnitude lower than the expected resistance of 10-m long section of pre-dart-leader channel having a radius of 3 cm and conductivity of 0.02 S/m.

## Acknowledgements

This work was supported in part by NSF grant AGS-1701484. The authors are grateful to W. Lyu for providing additional information on his high-speed camera records presented in Fig. 2 and to V.S. Syssoev and A.Yu. Kostinskiy for providing their unpublished photograph presented in Fig. 12 (top panel). Three anonymous reviewers provided useful comments on the manuscript.

## References


[1] A. Nag, V.A. Rakov, D. Tsalikis, J. Howard, C.J. Biagi, D. Hill, M.A. Uman, D.M. Jordan, Characteristics of the initial rising portion of near and far lightning return stroke electric field waveforms, Atmos. Res. 117 (2012) 71–77 Special Issue dedicated to the 30th International Conference on Lightning Protection (ICLP).

[2] M.D. Tran, V.A. Rakov, A study of the ground-attachment process in natural lightning with emphasis on its breakthrough phase, Springer Nat. Sci. Rep. 7 (2017) 13, https://doi.org/10.1038/s41598-017-14842-7 15761.

[3] M.D. Tran, V.A. Rakov, Supplementary Information to "A study of the ground-attachment process in natural lightning with emphasis on its breakthrough phase". Preprint submitted to Scientic Reports, 2017, 12 p.

[4] J. Howard, M.A. Uman, C. Biagi, D. Hill, J. Jerauld, V.A. Rakov, J. Dwyer, Z. Saleh, H. Rassoul, RF and X-ray source locations during the lightning attachment process, J. Geophys. Res. 115 (2010) D06204, , https://doi.org/10.1029/2009JD012055.

[5] J.D. Hill, M.A. Uman, D.M. Jordan, T. Ngin, W.R. Gamerota, J. Pilkey, J. Caicedo, The attachment process of rocket-triggered lightning dart-stepped leaders, J. Geophys. Res. Atmos. 121 (2016) 853–871, https://doi.org/10.1002/2015JD024269.

[6] A.Yu. Kostinskiy, V.S. Syssoev, N.A. Bogatov, E.A. Mareev, M.G. Andreev, M.U. Bulatov, L.M. Makal'sky, D.I. Sukharevsky, V.A. Rakov, Observations of the connection of positive and negative leaders in meter-scale electric discharges generated by clouds of negatively charged water droplets, J. Geophys. Res. Atmos. 121 (2016) 9756–9766.

[7] V.A. Rakov, M.A. Uman, Lightning: Physics and Effects, Cambridge University Press, New York, 2003.

[8] T.A. Warner, Upward leader development from tall towers in response to downward stepped leaders, Proceeding of the International Conference on Lightning Protection (ICLP) Cagliari (2010).

[9] W. Lu, L. Chen, Y. Ma, V.A. Rakov, Y. Gao, Y. Zhang, Q. Yin, Y. Zhang, Lightning attachment process involving connection of the downward negative leader to the lateral surface of the upward connecting leader, Geophys. Res. Lett. 40 (2013) 5531–5535, https://doi.org/10.1002/2013GL058060.

[10] W. Lu, Q. Qi, Y. Ma, L. Chen, X. Yan, V.A. Rakov, D. Wang, Y. Zhang, Two basic leader connection scenarios observed in negative lightning attachment process, High Volt (2016) 1–7, https://doi.org/10.1049/hve.2016.0002.

[11] R. Jiang, X. Qie, Z. Wang, H. Zhang, G. Lu, Z. Sun, M. Liu, X. Li, Characteristics of lightning leader propagation and ground attachment, J. Geophys. Res. Atmos. 120 (2015) 11988–12002.

[12] S. Visacro, M. Guimaraes, M.H. Murta Vale, Features of upward positive leaders initiated from towers in natural cloud-to-ground lightning based on simultaneous high-speed videos, measured currents, and electric fields, J. Geophys. Res. Atmos. 122 (2017) 12786–12800, https://doi.org/10.1002/2017JD027016.

[13] M.M.F. Saba, A.R. Paiva, C. Schumann, M.A.S. Ferro, K.P. Naccarato, J.C.O. Silva, F.V.C. Siqueira, D.M. Custódio, Lightning attachment process to common buildings, Geophys. Res. Lett. 44 (2017) 4368–4375, https://doi.org/10.1002/2017GL072796.

[14] D. Wang, V.A. Rakov, M.A. Uman, N. Takagi, T. Watanabe, D. Crawford, K.J. Rambo, G.H. Schnetzer, R.J. Fisher, Z.-I. Kawasaki, Attachment process in rocket-triggered lightning strokes, J. Geophys. Res. Atmos. 104 (1999) 2143–2150.

[15] C.J. Biagi, D.M. Jordan, M.A. Uman, J.D. Hill, W.H. Beasley, J. Howard, High-speed video observations of rocket-and-wire initiated lightning, Geophys. Res. Lett. 36 (2009), https://doi.org/10.1029/2009GL038525.

[16] V.B. Lebedev, G.G. Feldman, B.N. Gorin, Yu.V. Shcherbakov, V.S. Syssoev, V.A. Rakov, M.A. Uman, R.C. Olsen, Test of the image converter cameras complex for research of discharges in long air gaps and lightning, Proceeding of the 13th International Conference on Atmospheric Electricity vol. 7, (2007).

[17] Y.V. Shcherbakov, V.B. Lebedev, V.A. Rakov, G.G. Feldman, B.N. Gorin, V.S. Syssoev, M.A. Karpov, High-speed optical studies of the long sparks in very transient stages, in: Xun Hou, Wei Zhao, Baoli Yao (Eds.), Proceeding of the International Congress on High-Speed Photography and Photonics Proceedings of SPIE Vol. 6279 (2007).

[18] W.R. Gamerota, M.A. Uman, J.D. Hill, D.M. Jordan, Observations of corona in triggered dart-stepped leaders, Geophys. Res. Lett. 42 (2015) 1977–1983, https://doi.org/10.1002/2014GL062911.

[19] C.D. Weidman, E.P. Krider, The fine structure of lightning return stroke wave forms, J. Geophys. Res. 83 (1978) 6239–6247 (Correction 1982, 87, 7351).

[20] J. Jerauld, M.A. Uman, V.A. Rakov, K.J. Rambo, G.H. Schnetzer, Insights into the ground attachment process of natural lightning gained from an unusual triggered-lightning stroke, J. Geophys. Res. Atmos. 112 (2007), https://doi.org/10.1029/2006JD007682.

[21] V. Cooray, A model for negative first return strokes in lightning flashes, Phys. Scr. 55 (1997) 119–128.

[22] V. Cooray, R. Montano, V.A. Rakov, Model to represent negative and positive lightning first return strokes with connecting leaders, J. Electrostat. 60 (2004) 97–109.

[23] N.D. Murray, E.P. Krider, J.C. Willett, Multiple pulses in dE/dt and the fine structure of E during the onset of first return strokes in cloud-to-ocean lightning, Atmos. Res. 76 (2005) 455–480.

[24] V. Cooray, L. Arevalo, M. Rahman, J. Dwyer, H. Rassoul, On the possible origin of X-rays in long laboratory sparks, J. Atmos. Sol. Phys. 71 (2009) 1890–1898, https://doi.org/10.1016/j.jastp.2009.07.010.

[25] P.O. Kochkin, C.V. Nguyen, A.P.J. van Deursen, U. Ebert, Experimental study of hard X-rays emitted from metre-scale positive discharges in air, J. Phys. D Appl. Phys. 45 (2012) 425202, , https://doi.org/10.1088/0022-3727/45/42/425202.

[26] P.O. Kochkin, A.P.J. van Deursen, U. Ebert, Experimental study on hard X-rays emitted from metre-scale negative discharges in air, J. Phys. D Appl. Phys. 48 (2015) 025205, , https://doi.org/10.1088/0022-3727/48/2/025205.
[27] P. Kochkin, C. Köhn, U. Ebert, L. van Deursen, Analyzing X-ray emissions from meter-scale negative discharges in ambient air, Plasma Sources Sci. Technol. 25 (2016) 044002, , https://doi.org/10.1088/0963-0252/25/4/044002.
[28] M.A. Ihaddadene, S. Celestin, Increase of the electric field in head-on collisions between negative and positive streamers, Geophys. Res. Lett. 42 (2015) 5644–5651, https://doi.org/10.1002/2015GL064623.
[29] C. Köhn, O. Chanrion, T. Neubert, Electron acceleration during streamer collisions in air, Geophys. Res. Lett. 44 (2017) 2604–2613, https://doi.org/10.1002/2016GL072216.
[30] L. Babich, E. Bochkov, Numerical simulation of electric field enhancement at the contact of positive and negative streamers in relation to the problem of runaway electron generation in lightning and in long laboratory sparks, J. Phys. D Appl. Phys. 50 (2017) (2017) 7 455202.
[31] A. Luque, Radio frequency electromagnetic radiation from streamer collisions, J. Geophys. Res. Atmos. 122 (2017) 10497–10509, https://doi.org/10.1002/2017JD027157.
[32] M.A. Uman, D.K. McLain, Magnetic field of lightning return stroke, J. Geophys. Res. 74 (1969) 6899–6910, https://doi.org/10.1029/JC074i028p06899.
[33] R.H. Golde, The frequency of occurrence and the distribution of lightning flashes to transmission lines, Electr. Eng. 64 (12) (1945) 902–910, https://doi.org/10.1109/EE.1945.6441405.
[34] V.A. Rakov, A.O. Lutz, A new technique for estimating equivalent attractive radius for downward lightning flashes, Paper 2.2 Presented at 20th International Conference on Lightning Protection, Swiss Electronical Association (1990).
[35] V. Cooray, U. Kumar, F. Rachidi, C.A. Nucci, On the possible variation of the lightning striking distance as assumed in the IEC lightning protection standard as a function of structure height, Electr. Power Syst. Res. 113 (2014) 79–87, https://doi.org/10.1016/j.epsr.2014.03.017.
[36] A. Larsson, An experimental study of inhibited electrical discharges in air, J. Phys. D Appl. Phys. 31 (15) (1998) 1823, https://doi.org/10.1088/0022-3727/31/15/010.
[37] A.Yu. Kostinskiy, V.S. Syssoev, N.A. Bogatov, E.A. Mareev, M.G. Andreev, M.U. Bulatov, D.I. Sukharevsky, V.A. Rakov, Abrupt elongation (stepping) of negative and positive leaders culminating in an intense corona streamer burst: observations in long sparks and implications for lightning, J. Geophys. Res. Atmos. 123 (2018) 5360–5375, https://doi.org/10.1029/ 2017JD027997.
[38] A. Nag, V.A. Rakov, Parameters of electric field waveforms produced by positive lightning return strokes, IEEE Trans. EMC 56 (August (4)) (2014) 932–939, https://doi.org/10.1109/TEMC.2013.2293628.
[39] M. Rubinstein, F. Rachidi, M.A. Uman, R. Thottappillil, V.A. Rakov, C.A. Nucci, Characterization of vertical electric fields 500 m and 30 m from triggered lightning, J. Geophys. Res. 100 (1995) 8863–8872 .
[40] E.P. Krider, C.D. Weidman, R.C. Noggle, The electric field produced by lightning stepped leaders, J. Geophys. Res. 82 (1977) 951–960.
[41] V.A. Rakov, M.A. Uman, K.J. Rambo, M.I. Fernandez, R.J. Fisher, G.H. Schnetzer, R. Thottappillil, A. Eybert-Berard, J.P. Berlandis, P. Lalande, A. Bonamy, P. Laroche, A. Bondiou-Clergerie, New insights into lightning processes gained from triggered-lightning experiments in Florida and Alabama, J. Geophys. Res. 103 (1998) 14117–14130.
[42] J.D. Hill, J. Pilkey, M.A. Uman, D.M. Jordan, W. Rison, P.R. Krebhiel, M.I. Biggerstaff, P. Hyland, R. Blakeslee, Correlated lightning mapping array and radar observations of the initial stages of three sequentially triggered Florida lightning discharges, J. Geophys. Res. Atmos. 118 (2013) 8460–8481, https://doi.org/10.1002/jgrd.50660.
[43] B.N. Gorin, A.V. Shkilev, Development of the electric discharge in long gaps subjected to positive voltage impulses, Electricity (2) (1974) 29–38.
[44] B.N. Gorin, Mathematical modeling of the lightning return stroke, Elektrichestvo 4 (1985) 10–16.
[45] V.A. Rakov, Some inferences on the propagation mechanisms of dart leaders and return strokes, J. Geophys. Res. 103 (1998) 1879–1887.
[46] N.A. Bogatov, A.Yu. Kostinskiy, V.S. Syssoev, M.G. Andreev, M.U. Bulatov, D.I. Sukharevsky, E.A. Mareev, V.A. Rakov, Experimental investigation of the streamer zone of positive leader using the high-speed photography and microwave probing, J. Geophys. Res. Atmos. (2019) (to be submitted for publication).
[47] G. Maslowski, V.A. Rakov, A study of the lightning-channel corona sheath, J. Geophys. Res. 111 (2006) 16, https://doi.org/10.1029/2005JD006858 D14110.
[48] E.M. Bazelyan, B.N. Gorin, V.I. Levitov, Physical and Engineering Fundamentals of Lightning Protection, 223 pp Gidrometeoizdat, Leningrad, Russia, 1978.
[49] K.L. Cummins, E.P. Krider, M. Olbinski, R.L. Holle, A case study of lightning attachment to flat ground showing multiple unconnected upward leaders, Atmos. Res. 202 (2018) 169–174, https://doi.org/10.1016/j.atmosres.2017.11.007.
[50] A.J. Eriksson, Lightning and tall structures, Trans. South African IEE 69 (1978) 2–16.
[51] D.A. Petersen, W.H. Beasley, High-speed video observations of a natural negative stepped leader and subsequent dart-stepped leader, J. Geophys. Res. Atmos. 118 (119) (2013) 10–12, https://doi.org/10.1002/2013JD019910.